Author Manuscript

Author Manuscript

Author Manuscript

Author Manuscript

HHS Public Access

Author manuscript

Inhal Toxicol. Author manuscript; available in PMC 2016 August 01.

Published in final edited form as:

Inhal Toxicol. 2016 August ; 28(9): 383–392. doi:10.1080/08958378.2016.1179373.

Repeated Ozone Exposure Exacerbates Insulin Resistance And Activates Innate Immune Response In Genetically Susceptible Mice

Jixin Zhong[1,*], **Katryn Allen**[2], **Xiaoquan Rao**[1], **Zhekang Ying**[1], **Zachary Braunstein**[3], **Saumya R. Kankanala**[1], **Chang Xia**[1], **Xiaoke Wang**[1], **Lori A. Bramble**[2], **James G. Wagner**[2], **Ryan Lewandowski**[2], **Qinghua Sun**[4], **Jack R. Harkema**[2,*], and **Sanjay Rajagopalan**[1,*]

[1]Division of Cardiovascular Medicine, Department of Medicine, University of Maryland School of Medicine, Baltimore, Maryland, USA

[2]EPA Great Lakes Clean Air Research Center, Michigan State University, East Lansing, Michigan, USA

[3]Boonshoft School of Medicine, Wright State University, Dayton, Ohio, USA

[4]Davis Heart & Lung Research Institute, Department of Internal Medicine, The Ohio State University, Columbus, Ohio, USA

Abstract

Background—Inhaled ozone (O_3) has been demonstrated as a harmful pollutant and associated with chronic inflammatory diseases such as diabetes and vascular disorders. However, the underlying mechanisms by which O_3 mediates harmful effects are poorly understood.

Objectives—To investigate the effect of O_3 exposure on glucose intolerance, immune activation and underlying mechanisms in a genetically susceptible mouse model.

Methods—Diabetes-prone KK mice were exposed to filtered air (FA), or O_3 (0.5 ppm) for 13 consecutive weekdays (4 h/day). Insulin tolerance test (ITT) was performed following the last exposure. Plasma insulin, adiponectin, and leptin were measured by ELISA. Pathologic changes were examined by H&E and oil-red-o staining. Inflammatory responses were detected using flow cytometry and real-time PCR.

Results—KK mice exposed to O_3 displayed an impaired insulin response. Plasma insulin and leptin levels were reduced in O_3-exposed mice. Three-week exposure to O_3 induced lung inflammation and increased monocytes/macrophages in both blood and visceral adipose tissue. Inflammatory monocytes/macrophages increased both systemically and locally. CD4+ T cell

[*]Address for correspondence: Sanjay Rajagopalan (srajagopalan@medicine.umaryland.edu), or Jack R. Harkema (harkemaj@cvm.msu.edu), or Jixin Zhong (jzhong@medicine.umaryland.edu), 20 Penn St., HSF-II S012C, Baltimore, MD 21201 Tel: 410-706-3582; Fax: 410-706-3583.

AUTHORS' CONTRITUBIONS

JZ, KA, ZB, XR, and ZY performed the experiments and contributed to acquisition of data. JRH and SR designed the experiment and interpreted the results. QS, LAB, JGW, and RL contributed to O_3 exposure of the animals. The manuscript was written by JZ/KA and revised critically by JGW/JRH/SR. All authors read, corrected and approved the manuscript.

COMPETING INTERESTS

The authors declare no conflict of interests in this paper.

Author Manuscript Author Manuscript Author Manuscript Author Manuscript

activation was also enhanced by the exposure of O_3 although the relative percentage of CD4+ T cell decreased in blood and adipose tissue. Multiple inflammatory genes including CXCL-11, IFN-γ, TNFα, IL-12, and iNOS were up-regulated in visceral adipose tissue. Furthermore, the expression of oxidative stress-related genes such as *Cox4*, *Cox5a*, *Scd1*, *Nrf1*, and *Nrf2*, increased in visceral adipose tissue of O_3-exposed mice.

Conclusions—Repeated O_3 inhalation induces oxidative stress, adipose inflammation and insulin resistance.

Keywords

Air pollution; Ozone exposure; Insulin resistance; Inflammation; Oxidative stress

BACKGROUND

Ozone (O_3) is a reactive gas consisting of three oxygen atoms. The O_3 layer in the upper atmosphere (stratosphere) protects us from excessive ultraviolet radiation from sun. However, ambient O_3 at ground level (troposphere) is harmful to human health because of its highly oxidizing property. Although the underlying mechanisms are poorly understood, the adverse effect of O_3 on cardiovascular diseases has been well-established. Epidemiologic studies suggest an association between O_3 exposure and cardiovascular disease (Azevedo et al. 2011; Lee et al. 2003; Middleton et al. 2008; Ruidavets et al. 2005). Exposures as short as several hours might increase the incidence of adverse cardiovascular events (Rich et al. 2006). However, the role of O_3 exposure in another chronic disease, diabetes, is not fully illustrated. There was no direct evidence, until recently, showing the link between O_3 exposure and diabetes. Studies suggest O_3 inhalation induces insulin resistance in rats (Bass et al. 2013; Vella et al. 2015). Bass showed acute and sub-chronic exposures to O_3 induce glucose intolerance with a weaker effect in sub-chronic exposure (Bass et al. 2013). Vella et al. reported that overnight exposure to O_3 triggers insulin resistance by activating JNK pathway (Vella et al. 2015). Study from our group also suggests O_3 exposure induces inflammation in epicardial and perirenal adipose tissues in rats (Sun et al. 2013). Type 2 diabetes is a chronic disorder involving both genetic and environmental factors. The effect of O_3 exposure as an environmental risk factor on individuals genetically susceptible to diabetes is not clear.

Inflammation in peripheral tissues is closely associated with the development of insulin resistance and vascular dysfunction (Berg and Scherer 2005). Increased macrophage infiltration in the adipose tissue (from ~5% to 60%) is found in obesity (Weisberg et al. 2003), a major risk factor for the development of type 2 diabetes. mRNA transcripts as well as protein levels of inflammatory genes such as TNFα, IL-6, complement factor C3, and MCP-1 in adipose tissue are induced by diet-induced obesity (Kern et al. 2001; Shimomura et al. 1996; Xu et al. 2003). Suppression of inflammation such as drug treatment or genetic disruption of pro-inflammatory gene may reverse obesity-induced insulin resistance (Hundal et al. 2002; Shoelson et al. 2003; Yuan et al. 2001).

In the current study, we used the obesity-prone KK mouse which develops moderate degrees of obesity, insulin resistance and diabetes (Hayase et al. 1996; Matsuo et al. 1970). The KK

Author Manuscript Author Manuscript Author Manuscript Author Manuscript

mouse is an inbred strain established by Kondo et al. from Japanese native mice (Iwatsuka et al. 1970). KK mice with A^y mutation develop marked adiposity and hyperglycemia at early stage, while wild-type KK mice only develop moderate obesity and insulin resistance (Iwatsuka et al. 1970; Matsuo et al. 1970). The KK strain is sensitive to factors such as high fat diet and therefore is a useful model to study the pathogenesis, therapy, and prevention of obesity and diabetes (Hayase et al. 1996; Herberg and Coleman 1977; Matsuo et al. 1970). To investigate effects of O_3 inhalation on adipose inflammation and diabetes, changes in immune activation and oxidative stress in response to O_3 exposure were examined in adult male KK mice exposed to filtered air (FA) or O_3 in current study.

RESULTS

Pulmonary Inflammation Induced by O_3 Exposures

Bronchoalveolar Lavage Fluid (BALF)—KK mice exposed to O_3 had markedly greater (3x) inflammatory cells in the BALF (collected ~24 hours after the last exposure), as compared to mice exposed only to FA (controls). This was due to O_3-induced increases in lung lavaged monocytes/macrophages, neutrophils, eosinophils and lymphocytes (Figure 1A & 1B). O_3-exposed animals had 2.5 fold more monocytes/macrophages, 9.1 fold more neutrophils and 5.3 fold more lymphocytes, as compared to the BALF cells in filtered air-exposed mice (Figure 1B). Interestingly O_3-exposed mice had 31,211 ± 9,126 (mean ± standard error of the mean) eosinophils/ml of BALF, while no eosinophils were found in the BALF of air-exposed controls (Figure 1B).

Lung Histopathology—O_3-exposed KK mice had pulmonary histopathology that was restricted to centriacinar regions throughout the lung lobe compared to FA-exposed mice (Figure 2A & 2B). These O_3-induced lung lesions were morphologically characterized by marked thickening of terminal bronchioles and proximal alveolar ducts as a result of hyperplasia/hypertrophy of surface epithelium, intramural fibrosis, smooth muscle hypertrophy and a mixed inflammatory cell infiltrate (i.e., mononuclear cells, neutrophils and eosinophils; bronchiolitis/alveolitis). Conspicuous aggregates of monocytes/macrophages and lesser numbers of other inflammatory cells (i.e., neutrophils, eosinophils, and lymphocytes) were also present in centrinacinar airspaces. No exposure-related histopathology was found in the lungs of KK mice exposed only to filtered air (Figure 2A).

O_3 Inhalation Induced Insulin Tolerance in Insulin Resistant KK Mice

ITT was performed to evaluate the impact of O_3 inhalation on insulin sensitivity of KK mice. As shown in figure 3A, there were no differences in body weight compared to control before and after 13 days of O_3 exposure in KK mice. Although no significant difference in fasting blood glucose was observed between FA- and O_3-exposed animals (Figure 3B, 347.3 ± 8.9 mg/dL vs. 356.6 ± 32.1 mg/dL for FA vs. O_3), three-week O_3 exposure significantly impaired insulin sensitivity in KK mice (Figure 3C & 3D; Area under curve: 28413.4 ± 2291.2 vs. 42804.4 ± 3744.6 for FA vs. O_3, $p<0.05$). Fasting plasma insulin levels were lower in O_3-exposed mice (4.5 ± 0.6 ng/mL vs. 2.7 ± 0.4 ng/mL for FA vs. O_3, $p<0.05$, Figure 3E). Consistently, fasting plasma leptin level (14.8 ± 1.8 ng/mL vs. 8.3 ± 0.7 ng/mL

Author Manuscript Author Manuscript Author Manuscript Author Manuscript

for FA vs. O_3, $p<0.05$, Figure 3F) and HOMA-beta (152.1 ± 16.1 vs. 91.7 ± 21.8 for FA vs. O_3, $p<0.05$, Figure 3G) were also reduced after O_3 exposure in KK mice.

Effect of O_3 Exposure on Immune Cell Population in Blood and Adipose Tissue

Animals were sacrificed after 3-week exposure to FA or O_3 and blood was collected for the isolation of white blood cells. To investigate the impact of O_3 inhalation on immune response, macrophage and $CD4^+$ T cell population were quantified using flow cytometry. Monocytes were characterized by the expression CD11b and F4/80 in mice (Geissmann et al. 2003). As depicted in figure 4A, $CD11b^+$ $F4/80^+$ monocytes increased in blood (6.5 ± 0.1% vs. 7.9 ± 0.6% for FA vs. O_3) although no statistical significance was observed ($p=0.06$). CD4+ T cell percentage in blood was lower in O_3-exposed mice (14.3 ± 0.6% vs. 10.8 ± 0.6% for FA vs. O_3, $p=0.001$, Figure 4B). Consistently, infiltration of adipose tissue macrophage (ATM) increased in epididymal fat of KK mice exposed to O_3 (37.9 ± 1.2% vs. 44.3 ± 2.1% for FA vs. O_3, $p=0.02$, Figure 4C) and percentage of CD4+ T cell decreased in epididyma fat of O_3-exposed KK mice (1.2 ± 0.08% vs. 0.9 ± 0.08% for FA vs. O_3, $p=0.04$, Figure 4D).

Impact of O_3 Inhalation on Inflammatory Activation of Monocytes/T cells in Blood

Next we detected the activation of monocytes and $CD4^+$ T cells in the blood of O_3-exposed KK mice. Gr-1^{low} $7/4^{high}$ inflammatory monocytes were significantly increased in the circulation of KK mice exposed to O_3 (11.0 ± 1.3% vs. 19.4 ± 0.9% for FA vs. O_3, $p<0.001$, Figure 5A). To confirm this result, we used another marker Ly-6C to identify inflammatory monocytes. Consistently, Ly-$6C^+$ monocyte level in circulation was higher in O_3-exposed mice compared with that in FA-exposed mice (13.6 ± 1.4% vs. 18.9 ± 0.8% for FA vs. O_3, $p=0.006$, Figure 5B). Interestingly, the activated $CD4^+$ T cells ($CD4^+$ $CD62L^-$) also increased after O_3 exposure (85.4 ± 0.7% vs. 92.0 ± 1.0% for FA vs. O_3, $p<0.001$, Figure 5C).

Effect of O_3 Exposure on Liver Lipid Metabolism

As depicted in figure 6A, KK mice exposed to O_3 and FA had similar liver weights. H&E staining shows normal liver architecture and morphology in mice exposed to O_3 (Figure 6B). To investigate whether O_3 exposure affects hepatic lipid content, liver frozen sections were used for Oil-Red-O staining. As shown in figure 6C, similar levels of lipid content were observed in liver of mice exposed to FA and O_3.

Impact of O_3 Inhalation on Inflammatory Activation of Monocytes/T cells in Adipose Tissue

To investigate inflammatory cell infiltration in visceral adipose tissue, epididymal fat tissues from exposed mice were used for the H&E staining and Mac-1 immunofluorescence staining. More crown-like structures (infiltration of inflammatory cells) were observed in the epididymal fat of O_3-exposed mice (Figure 7A & 7B). Consistent with the observations in blood, infiltration of inflammatory macrophages in visceral adipose tissue was enhanced by O_3 exposure. As shown in figure 7C, percentage of Gr-1^{low} $7/4^{high}$ macrophage increased in the epididymal fat of O_3-exposed mice (2.8 ± 0.4% vs. 6.3 ± 1.1% for FA vs. O_3, $p=0.02$,). Ly-$6C^+$ macrophage infiltration in the epididymal fat of O_3-exposed mice is also higher than

Author Manuscript Author Manuscript Author Manuscript Author Manuscript

that of mice exposed to FA (1.5 ± 0.2% vs. 2.1 ± 0.2% for FA vs. O_3, p=0.04, Figure 7D). There was also an increased activation of $CD4^+$ T cell in the adipose tissue of O_3-exposed KK mice (76.8 ± 2.3% vs. 88.8 ± 6.1% for FA vs. O_3, p<0.001, Figure 7E).

Effect of O_3 Exposure on Inflammatory Gene Expression in Visceral Adipose Tissue

To further investigate the impact of O_3 inhalation on immune activation in adipose tissue, we next detected the mRNA expression level of chemokines, pro-inflammatory cytokines, and inflammatory genes in visceral adipose tissue. No significant difference in CCL-5, CXCL-12, CXCL-9, MCP-1, RORγ, T-bet and IL-6 were observed between FA- and O_3-exposed mice (Figure 8). Expression of CXCL-11 was increased by 8.5-fold in animals exposed to O_3 (1.0 ± 0.22 vs. 8.5 ± 2.63 for FA vs. O_3, p=0.02, Figure 8A). There were also a 5.4-fold increase of iNOS (1.0 ± 0.39 vs. 5.4 ± 1.26 for FA vs. O_3, p=0.007, Figure 8B), 2.8-fold increase of IFN-γ (1.0 ± 0.23 vs. 2.8 ± 0.73 for FA vs. O_3, p=0.045, Figure 8B), 4.1-fold increase of IL-12 (1.0 ± 0.40 vs. 4.1 ± 1.10 for FA vs. O_3, p=0.026, Figure 8B), 11.5-fold increase of TNFα (1.0 ± 0.24 vs. 11.5 ± 4.24 for FA vs. O_3, p=0.039, Figure 8B) and 2.7-fold increase of CD56 (1.0 ± 0.24 vs. 2.7 ± 0.74 for FA vs. O_3, p=0.033, Figure 8B).

O_3 Exposure Promotes Oxidative Stress

To investigate whether oxidative stress plays a role in O_3 exposure, we detected the expression of genes involved in oxidative stress. As depicted in figure 9, multiple oxidative stress-related genes including *Cox4* (1.0 ± 0.16 vs. 2.9 ± 0.71 for FA vs. O_3, p=0.021), *Cox5a* (1.0 ± 0.16 vs. 2.0 ± 0.34 for FA vs. O_3, p=0.016), *Scd1* (1.0 ± 0.18 vs. 3.1 ± 0.93 for FA vs. O_3, p=0.041), *Nrf1* (1.0 ± 0.24 vs. 2.6 ± 0.52 for FA vs. O_3, p=0.014), and *Nrf2* (1.0 ± 0.17 vs. 1.8 ± 0.36 for FA vs. O_3, p=0.045) were up-regulated by the exposure of O_3. The expression of *Gclm* increased by 1.1-fold although it was not statistically significant (p=0.053). No Significant differences in *Cox1*, *Cox7a*, and *Nqo1* between FA and O_3 were observed (Figure 9).

DISCUSSION

The effects of O_3 exposure on cardiometabolic diseases are not fully understood. Although several studies have indicated acute (hours to 2 days) and chronic/sub-chronic (months) O_3 exposure may induce insulin resistance (Bass et al. 2013; Sun et al. 2013; Vella et al. 2015), the effect of sub-acute exposure to O_3 on insulin sensitivity is not clear. In addition, the effect of O_3 exposure on diabetes susceptible individuals has not been reported. In the current study, we provided direct evidence showing 13 consecutive weekdays of O_3 exposure promotes insulin resistance in mice genetically susceptible to diabetes. Repeated O_3 exposure also enhanced oxidative stress and adipose tissue inflammation.

It has been reported that acute exposure to O_3 elevated fasting blood glucose level in rats (Miller et al. 2015; Miller et al. 2016). In our study, however, there was a similar fasting blood glucose level in FA- and O_3-exposed KK mice. This is probably because the responsiveness to O_3 is different in different genetic background and the effect of O_3 may vary when exposed for different durations. However, we did observed a significant adverse effect of O_3 inhalation on insulin sensitivity. Three-week O_3 inhalation exacerbated the

Author Manuscript Author Manuscript Author Manuscript Author Manuscript

response to insulin in KK mice. HOMA-beta, an index for beta cell insulin secretory function (Matthews et al. 1985; Wallace et al. 2004), was also reduced in KK mice exposed to O_3. In consistency with our results, a recent study reported that exposure to O_3 impaired insulin sensitivity in the skeletal muscle of rats (Vella et al. 2015). Vella and coworkers demonstrated that overnight O_3 exposure triggered insulin resistance by activating JNK pathway (Vella et al. 2015). Interestingly, in our study, the fasting plasma insulin and leptin levels were lower in mice expose to O_3. This suggests that O_3-induced oxidative stress and systemic inflammation impair the function of islet cells and adipocytes.

Inflammation has long been associated with cardiometabolic diseases (Despres 2012; Ross 1999; Shah et al. 2008; Taube et al. 2012; Van Eeden et al. 2012). Cardiometabolic diseases such as atherosclerosis and diabetes are parallel with increase of multiple inflammatory changes. For instance, atherosclerotic lesions are dominated by immune cells at the early stage. The activation of inflammation accelerates the progression of lesions and elicits acute coronary syndromes (Hansson 2005). Obesity-induced diabetes is also characterized by chronic low grade inflammation in the peripheral tissues (Luft et al. 2013; Wellen and Hotamisligil 2005). To investigate whether O_3 inhalation has an impact on inflammation, KK mice were exposed to O_3or FA for 13 days over 3 weeks. O_3 exposure increased inflammatory cells including monocyte/macrophage, lymphocyte, eosinophil, and neutrophil in the BALF by 2.5- to 10-fold. Lung histological examination confirmed the inflammation in the centriacinar regions throughout the lung lobe in O_3-exposed KK mice. The inflammatory markers on circulating monocyte and adipose tissue macrophages increased upon exposure to O_3. Furthermore, the percentage of monocyte/macrophage was also elevated in mice with O_3 exposure. However, the percentage of $CD4^+$ T cell decreased in O_3-exposed mice. This is probably caused by the increase of macrophage population. Although percentage of $CD4^+$ T cells in the circulation was reduced, the activation of $CD4^+$ T cell ($CD4^+CD62L^-$) increased in O_3-exposed KK mice. All these results suggest that O_3 inhalation promotes inflammatory response in both circulation and adipose tissue, and might play a role in the development of insulin resistance and diabetes.

Realtime PCR analysis indicated that there was an increase of multiple inflammatory genes in visceral adipose tissue such as CXCL-11, iNOS, IFN-γ, IL-12, and TNFα. CD56, a marker for NK cells, also increased in O_3-exposed mice. This indicates NK cells might at least in part contribute to the increase of inflammatory cytokines such as IFN-γ and TNFα in O_3 exposure. The increase of type 1 cytokines such as IFN-γ and IL-12 in visceral fat may induced the classical activation of adipose tissue macrophages. Classically activated macrophages highly express iNOS and TNFα, and is confirmed to be major contributor for adipose inflammation and insulin resistance (Olefsky and Glass 2010; Winer and Winer 2012). Deficiency of IFN-γ improves insulin resistance and switch macrophage activation towards alternative activation (O'Rourke et al. 2012). CXCL-11, also known as Interferon-inducible T Cell Alpha Chemoattractant (I-TAC) or Interferon-gamma-inducible protein 9 (IP-9), is a chemokine belonging to the CXC chemokine family. Studies have shown CXCL-11 can be induced by IFN-γ through a STAT3-dependent pathway (Yang et al. 2007). The increase of CXCL-11 is probably caused by the enhancement of IFN-γ and may further promote the recruitment of activated T cells into the visceral fat.

Author Manuscript Author Manuscript Author Manuscript Author Manuscript

Previous studies including those from our group have demonstrated oxidative stress is an important mechanism underlying inflammation induced by air pollutants such as $PM_{2.5}$ (Grevendonk et al. 2016; Rajagopalan and Brook 2012; Sun et al. 2010; Xu et al. 2010; Xu et al. 2011) and cigarette smoking (Carnevali et al. 2003; Mons et al. 2016). $PM_{2.5}$ exposure was associated with oxidative stress in various tissues including lung, liver, white adipose tissue, and brown adipose tissue (Laing et al. 2010; Rajagopalan and Brook 2012; Xu et al. 2010; Xu et al. 2011). Exposure to $PM_{2.5}$ increased phosphorylation of p47, a key cytosolic subunit of NADPH oxidase, in visceral adipose tissue. $p47^{phox-/-}$ mice were protected from $PM_{2.5}$-induced adverse effects such as impairment in insulin resistance, vascular function, and visceral inflammation (Xu et al. 2010). To investigate whether oxidative stress is also involved in O_3-induced inflammation and insulin resistance, we detected genes involved in the oxidative stress. *Nrf1* and *Nrf2*, both of which are master regulator of oxidative stress signaling (Ma 2013; Schultz et al. 2010), were up-regulated by O_3 exposure. During the process of oxidative stress, the Nrf proteins are up-regulated and induce the expression of a variety of antioxidant and xenobiotic-metabolizing enzymes (Biswas and Chan 2010). Cytochrome-c oxidase (COX) also regulates radical production and oxidative stress by controlling mitochondrial respiration (Kadenbach et al. 2004; Srinivasan and Avadhani 2012). In our study, we observed an up-regulation of *Cox4* and *Cox5a* mRNA in the adipose tissue of O_3-exposed mice. The proteins encoded by *Gclm* and *Scd1* are rate-limiting enzymes in glutathione synthesis and fatty acid metabolism respectively, and are both important regulators in oxidative stress (Lim et al. 2015; Liu et al. 2011; Yang et al. 2002). The expressions of *Gclm* and *Scd1* both increased in visceral adipose tissue after exposure to O_3. These results suggest exposure to O_3 may induce oxidative stress in visceral adipose tissue.

In this study, we perform a short-term whole body exposure of the diabetes prone KK mice to O_3 or filtered air. We demonstrated that short-term exposure to O_3 (4h/day, 13 days) significantly impaired insulin sensitivity, accompanied by enhanced inflammation and oxidative stress in visceral adipose tissue. This study suggested that O_3, as an important component of polluted air, has great potential to promote progress of inflammatory response and type 2 diabetes.

CONCLUSIONS

O_3 exposure exacerbates insulin resistance in diabetes-prone mice by triggering oxidative stress and systemic/local inflammatory response.

MATERIALS AND METHODS

Animals

Japanese KK mice were purchased from The Jackson Laboratory (Stock # 002468, KK-a/a genotype, Bar Harbor, ME) and were allowed to acclimate for two weeks before beginning inhalation exposure protocols. All procedures of this study were approved by the Institutional Animal Care and Use Committees at Michigan State University and the Ohio State University. Michigan State University is an AAALAC accredited institution.

Author Manuscript Author Manuscript Author Manuscript Author Manuscript

O_3 Exposure

Inhalation exposures and tissue collection procedures were conducted at Michigan State University. Mice (8/group) were exposed to filtered air (FA), or O_3 (O_3; 0.5 ppm target) for 13 consecutive weekdays (Monday to Friday, 4 h/day). Choice of the O_3 exposure regimen was made on previously reported rodent studies in our group and others (Katre et al. 2011; Last et al. 2004; Sun et al. 2013; Wagner et al. 2014; Ying et al. 2016). The magnitude of O_3-induced airway epithelial injury and inflammation are exposure (e.g., concentration, time, and frequency) and species dependent. It has been experimentally documented that it takes approximately 4 to 5 times the concentration of O_3 to induce pulmonary inflammation in laboratory rodents that is similar to that in exercising human subjects under similar controlled acute exposure conditions (Hatch et al. 2013; Hatch et al. 1994). The airborne concentration that was chosen for this exposure was equivalent to an exercising human exposure of 0.15 ppm or approximately twice the concentration of the current U.S. National Ambient Air Quality Standard (NAAQS) for O_3 (0.070 ppm). Mice were housed individually in stainless steel wire cages, and exposed to O_3 in whole body inhalation exposure chambers (H-1000; Lab Products Marywood, NJ). O_3 was generated with an OREC 03V1-Clone O_3 generator (Ozone Research and Equipment Corp., AZ) using compressed air as a source of oxygen, and monitored with a Dasibi 1003 AH ambient air O_3 monitor (Dasibi Environmental Corp., Glendale, CA). The actual chamber concentrations were 0.49586 ± 0.000926 ppm (mean ± SEM), and were highly consistent throughout the 13-day study. Food was removed during exposures. All mice were sacrificed 22 h after the last exposure.

Intraperitoneal Insulin Tolerance Test (IPITT)

Two hours after the last exposure (fasted for 6 hours), baseline blood glucose and body weights were measured. Animals received an insulin injection of 0.75U/kg body weight, blood was obtained by tail vein puncture at 15, 30, 60, 90, 120, and 130 min post injection. Glucose was measured with a Bayer Contour® glucometer. Food was returned to the animals at completion of the test.

Necropsy

Six hours prior to necropsy animals were again fasted. Approximately, twenty-two hours after the last exposure, mice were deeply anesthetized with sodium pentobarbital (50 mg/kg, i.p.), blood was collected from the ascending vena cava for plasma isolation, and then mice were exsanguinated by cutting the abdominal.

Bronchoalveolar Lavage & Lung Histopathology

Immediately after death, the trachea was cannulated and the heart and lungs were excised *en bloc*. A volume of 0.8 mL sterile saline was instilled through the tracheal cannula and withdrawn to recover bronchoalveolar lavage fluid (BALF). A second intratracheal saline lavage was performed and the collected BALF was combined with the first sample for analysis. Total number of cells in the collected BALF was estimated using a hemocytometer. Cytological slides were prepared by centrifugation (Shandon cytospin 3) and stained with

Author Manuscript Author Manuscript Author Manuscript Author Manuscript

Diff-Quick and differential cell counts for neutrophils, eosinophils, macrophages/monocytes, and lymphocytes were assessed from a total of 200 cells.

After the BALF was collected, the left lung lobe was intratracheally fixed with neutral-buffered formalin at a constant pressure (30 cm H_2O) for 2 h and then stored in a large volume of the same fixative until further tissue processing for light microscopy. The right caudal lobe was removed for RT-PCR. Twenty-four hours later, two sections were excised at the level of the 5th and 11th airway generation along the main axial airway (G5 and G11), to sample proximal and distal bronchiolar airways, respectively. Tissue blocks were then embedded in paraffin and 5- to 6-μm thick sections were cut from the anterior surface. Lung sections were stained with hematoxylin and eosin (H&E) for routine light microscopic examination and with Alcian Blue (pH 2.5)/Periodic Acid–Schiff (AB/PAS) for identification of intraepithelial neutral and acidic mucosubstances in pulmonary bronchiolar epithelium.

Adipose Stromal Vascular Fraction (SVF) isolation

At necropsy, the stromal vascular fraction (SVF) was immediately isolated from epididymal fat by digesting it with collagenase type II as described previously (Zhong et al. 2013). Briefly, visceral adipose tissues were extensively rinsed in PBS, minced and then digested with 1 mg/mL collagenase type II from *Clostridium histolyticum* (Sigma, St. Louis, MO) at 37°C water bath with a shaking speed of 140 rpm for 30 min. The digesta was then filtered through a 100 μm nylon cell strainer (BD Biosciences, San Jose, CA), followed by centrifugation at 300 × g for 5 min. The cells were then lyzed with 1× RBC lysing buffer (Sigma, St. Louis, MO) to get rid of contaminating red blood cells. After wash with PBS, the resulting pellet (SVF) was resuspended with PBS and analyzed with flow cytometry.

Adipose Histology

Epididymal fat tissues from exposed mice were fixed in 10% Neutral Buffered Formalin and embedded in paraffin. Paraffin-embedded tissue sections (8 μm) were subjected to hematoxylin and eosin (H&E) staining as described previously (Zheng et al. 2013). For detection of Mac-1α, some sections were blocked in 2% BSA for 1 h after incubation in 1× Retrieve-All Antigen Unmasking Solution (Covance, Vienna, VA). Sections were then incubated with Mac-1α (Clone: M1/70) primary antibody (Biolegend, San Diego, CA) overnight at 4°C, followed by incubation with Texas Red-labeled anti-rat secondary antibody. After mounting, slides were kept at 4°C until imaging. Images were captured using Zeiss LSM 510 inverted confocal.

Liver Oil-Red-O Staining

Oil-Red-O staining was performed as described previously(Liu et al. 2014). Briefly, hepatic frozen sections were stained with Oil-Red-O working solution (5mg/mL Oil-Red-O stock solution: ddH_2O = 3 : 2), followed by staining with haematoxylin.

Adipose Flow Cytometry

All antibodies used in flow cytometry were purchased from BioLegend, San Diego, CA (CD4, clone GK1.5; CD11b, clone M1/70; CD62L, clone MEL-14; Ly6c, clone HK1.4;

Author Manuscript Author Manuscript Author Manuscript Author Manuscript

Gr-1, clone RB6-8C5), AbD Serotec, Raleigh, NC (Ly-6B.2, Clone 7/4), or BD, San Jose, CA (CD16/32 Fcγ III/II receptor, clone 2.4G2). 100 μL cell suspension containing 1×10^6 cells were incubated with anti-mouse CD16/32 Fcγ III/II receptor (BD, San Jose, CA) at 4°C for 15 min. Cells were then stained with indicated antibodies at 4°C for 30 min. After washes with PBS, cells were then analyzed on a BD LSRII cytometer (BD, San Jose, CA).

Adipose Real-time PCR

Total RNAs were isolated from epididymal fat of FA or O_3-exposed mice using Trizol® Reagent (Life Technologies, Grand Island, NY). cDNA were synthesized from mRNA using a High Capacity cDNA Reverse Transcriptase Kit (Life Technologies, Grand Island, NY) according to the manufacturer's instruction. The quantitative real-time PCR analysis was performed on a light 480 real-time PCR System (Roche Applied Science, Indianapolis, IN) following the standard procedure. Target genes were amplified using a LightCycler® 480 SYBR Green I Master kit (Roche Applied Science, Indianapolis, IN). The primers used for real-time PCR are described in Table 1. Fold changes of mRNA levels were determined after normalization to internal control β-actin RNA levels.

Plasma ELISA

After overnight fasting, plasma was prepared from anticoagulated (K2EDTA) whole blood by centrifugation at 2000 g for 15 min. Plasma insulin, adiponectin, and leptin levels were measured using a Mouse Insulin ELISA kit (Crystal Chem Inc., Downers Grove, IL), Quantikine® Mouse Leptin Immunoassay kit, and Quantikine® Mouse Leptin Immunoassay kit (R&D Systems, Minneapolis, MN) as instructed by the manufacturer.

Statistical Analysis

Data are expressed as mean ± SEM. The results were analyzed by unpaired t test using Graphpad Prism v5.0 (GraphPad Software, San Diego, CA). A P value of < 0.05 was considered as statistically significant.

Acknowledgments

This publication was made possible by US EPA grant (R834797 to Drs. Rajagopalan and Harkema). SR was supported by RO1 ES015146 and R01 ES017290. JZ was supported by grants from NIDDK/NIH (K01 DK105108), AHA (15SDG25700381 and 13POST17210033) and Mid-Atlantic Nutrition Obesity Research Center (NORC Pilot and Feasibility Program). XW was supported by a grant from Natural Science Foundation of Jiangsu Province (13KJB330007).

References

Anenberg SC, Horowitz LW, Tong DQ, West JJ. An estimate of the global burden of anthropogenic ozone and fine particulate matter on premature human mortality using atmospheric modeling. Environmental health perspectives. 2010; 118(9):1189–95. DOI: 10.1289/ehp.0901220 [PubMed: 20382579]

Azevedo JM, Goncalves FL, de Fatima Andrade M. Long-range ozone transport and its impact on respiratory and cardiovascular health in the north of Portugal. Int J Biometeorol. 2011; 55(2):187–202. DOI: 10.1007/s00484-010-0324-2 [PubMed: 20593201]

Bass V, Gordon CJ, Jarema KA, et al. Ozone induces glucose intolerance and systemic metabolic effects in young and aged Brown Norway rats. Toxicology and applied pharmacology. 2013; 273(3): 551–60. DOI: 10.1016/j.taap.2013.09.029 [PubMed: 24103449]

Author Manuscript Author Manuscript Author Manuscript Author Manuscript

Bell ML, McDermott A, Zeger SL, Samet JM, Dominici F. Ozone and short-term mortality in 95 US urban communities, 1987–2000. JAMA. 2004; 292(19):2372–8. DOI: 10.1001/jama.292.19.2372 [PubMed: 15547165]

Berg AH, Scherer PE. Adipose tissue, inflammation, and cardiovascular disease. Circ Res. 2005; 96(9):939–49. DOI: 10.1161/01.RES.0000163635.62927.34 [PubMed: 15890981]

Biswas M, Chan JY. Role of Nrf1 in antioxidant response element-mediated gene expression and beyond. Toxicology and applied pharmacology. 2010; 244(1):16–20. S0041-008X(09)00324-X [pii]. DOI: 10.1016/j.taap.2009.07.034 [PubMed: 19665035]

Brook RD, Rajagopalan S. Chronic air pollution exposure and endothelial dysfunction: what you can't see--can harm you. J Am Coll Cardiol. 2012; 60(21):2167–9. DOI: 10.1016/j.jacc.2012.08.974 [PubMed: 23103034]

Brook RD, Rajagopalan S, Pope CA 3rd, et al. Particulate matter air pollution and cardiovascular disease: An update to the scientific statement from the American Heart Association. Circulation. 2010; 121(21):2331–78. DOI: 10.1161/CIR.0b013e3181dbece1 [PubMed: 20458016]

Carnevali S, Petruzzelli S, Longoni B, et al. Cigarette smoke extract induces oxidative stress and apoptosis in human lung fibroblasts. Am J Physiol Lung Cell Mol Physiol. 2003; 284(6):L955–63. 00466.2001 [pii]. DOI: 10.1152/ajplung.00466.2001 [PubMed: 12547733]

Chang HH, Zhou J, Fuentes M. Impact of climate change on ambient ozone level and mortality in southeastern United States. Int J Environ Res Public Health. 2010; 7(7):2866–80. DOI: 10.3390/ijerph7072866 [PubMed: 20717546]

Despres JP. Abdominal obesity and cardiovascular disease: is inflammation the missing link? Can J Cardiol. 2012; 28(6):642–52. DOI: 10.1016/j.cjca.2012.06.004 [PubMed: 22889821]

Foster WM, Brown RH, Macri K, Mitchell CS. Bronchial reactivity of healthy subjects: 18–20 h postexposure to ozone. J Appl Physiol. 2000; 89(5):1804–10. [PubMed: 11053329]

Geissmann F, Jung S, Littman DR. Blood monocytes consist of two principal subsets with distinct migratory properties. Immunity. 2003; 19(1):71–82. [PubMed: 12871640]

Grevendonk L, Janssen BG, Vanpoucke C, et al. Mitochondrial oxidative DNA damage and exposure to particulate air pollution in mother-newborn pairs. Environ Health. 2016; 15(1):10. [pii]. doi: 10.1186/s12940-016-0095-2 [PubMed: 26792633]

Hansson GK. Inflammation, atherosclerosis, and coronary artery disease. N Engl J Med. 2005; 352(16):1685–95. DOI: 10.1056/NEJMra043430 [PubMed: 15843671]

Hatch GE, McKee J, Brown J, et al. Biomarkers of Dose and Effect of Inhaled Ozone in Resting versus Exercising Human Subjects: Comparison with Resting Rats. Biomark Insights. 2013; 8:53–67. bmi-8-2013-053 [pii]. DOI: 10.4137/BMI.S11102 [PubMed: 23761957]

Hatch GE, Slade R, Harris LP, et al. Ozone dose and effect in humans and rats. A comparison using oxygen-18 labeling and bronchoalveolar lavage. American journal of respiratory and critical care medicine. 1994; 150(3):676–83. DOI: 10.1164/ajrccm.150.3.8087337 [PubMed: 8087337]

Hayase M, Ogawa Y, Katsuura G, Shintaku H, Hosoda K, Nakao K. Regulation of obese gene expression in KK mice and congenic lethal yellow obese KKAy mice. Am J Physiol. 1996; 271(2 Pt 1):E333–9. [PubMed: 8770028]

Herberg L, Coleman DL. Laboratory animals exhibiting obesity and diabetes syndromes. Metabolism. 1977; 26(1):59–99. [PubMed: 834144]

Hundal RS, Petersen KF, Mayerson AB, et al. Mechanism by which high-dose aspirin improves glucose metabolism in type 2 diabetes. J Clin Invest. 2002; 109(10):1321–6. DOI: 10.1172/JCI14955 [PubMed: 12021247]

Iwatsuka H, Shino A, Suzuoki Z. General survey of diabetic features of yellow KK mice. Endocrinol Jpn. 1970; 17(1):23–35. [PubMed: 5468422]

Jerrett M, Burnett RT, Pope CA 3rd, et al. Long-term ozone exposure and mortality. N Engl J Med. 2009; 360(11):1085–95. DOI: 10.1056/NEJMoa0803894 [PubMed: 19279340]

Kadenbach B, Arnold S, Lee I, Huttemann M. The possible role of cytochrome c oxidase in stress-induced apoptosis and degenerative diseases. Biochim Biophys Acta. 2004; 1655(1–3):400–8. S0005272803002020 [pii]. DOI: 10.1016/j.bbabio.2003.06.005 [PubMed: 15100056]

Author Manuscript Author Manuscript Author Manuscript Author Manuscript

Katre A, Ballinger C, Akhter H, et al. Increased transforming growth factor beta 1 expression mediates ozone-induced airway fibrosis in mice. Inhalation toxicology. 2011; 23(8):486–94. DOI: 10.3109/08958378.2011.584919 [PubMed: 21689010]

Kern PA, Ranganathan S, Li C, Wood L, Ranganathan G. Adipose tissue tumor necrosis factor and interleukin-6 expression in human obesity and insulin resistance. Am J Physiol Endocrinol Metab. 2001; 280(5):E745–51. [PubMed: 11287357]

Laing S, Wang G, Briazova T, et al. Airborne particulate matter selectively activates endoplasmic reticulum stress response in the lung and liver tissues. Am J Physiol Cell Physiol. 2010; 299(4):C736–49. DOI: 10.1152/ajpcell.00529.2009 [PubMed: 20554909]

Last JA, Ward R, Temple L, Kenyon NJ. Ovalbumin-induced airway inflammation and fibrosis in mice also exposed to ozone. Inhalation toxicology. 2004; 16(1):33–43. XF7WQ3163TTWRRXE [pii]. DOI: 10.1080/08958370490258237 [PubMed: 14744663]

Lee JT, Kim H, Cho YS, Hong YC, Ha EH, Park H. Air pollution and hospital admissions for ischemic heart diseases among individuals 64+ years of age residing in Seoul, Korea. Arch Environ Health. 2003; 58(10):617–23. DOI: 10.3200/AEOH.58.10.617-623 [PubMed: 15562633]

Lim J, Nakamura BN, Mohar I, Kavanagh TJ, Luderer U. Glutamate Cysteine Ligase Modifier Subunit (Gclm) Null Mice Have Increased Ovarian Oxidative Stress and Accelerated Age-Related Ovarian Failure. Endocrinology. 2015; 156(9):3329–43. DOI: 10.1210/en.2015-1206 [PubMed: 26083875]

Liu C, Xu X, Bai Y, et al. Air pollution-mediated susceptibility to inflammation and insulin resistance: influence of CCR2 pathways in mice. Environmental health perspectives. 2014; 122(1):17–26. DOI: 10.1289/ehp.1306841 [PubMed: 24149114]

Liu X, Strable MS, Ntambi JM. Stearoyl CoA desaturase 1: role in cellular inflammation and stress. Adv Nutr. 2011; 2(1):15–22. 000125 [pii]. DOI: 10.3945/an.110.000125 [PubMed: 22211186]

Luft VC, Schmidt MI, Pankow JS, et al. Chronic inflammation role in the obesity-diabetes association: a case-cohort study. Diabetol Metab Syndr. 2013; 5(1):31.doi: 10.1186/1758-5996-5-31 [PubMed: 23806173]

Ma Q. Role of nrf2 in oxidative stress and toxicity. Annu Rev Pharmacol Toxicol. 2013; 53:401–26. DOI: 10.1146/annurev-pharmtox-011112-140320 [PubMed: 23294312]

Matsuo T, Shino A, Iwatsuka H, Suzuoki Z. Induction of overt diabetes in KK mice by dietary means. Endocrinol Jpn. 1970; 17(6):477–88. [PubMed: 4931786]

Matthews DR, Hosker JP, Rudenski AS, Naylor BA, Treacher DF, Turner RC. Homeostasis model assessment: insulin resistance and beta-cell function from fasting plasma glucose and insulin concentrations in man. Diabetologia. 1985; 28(7):412–9. [PubMed: 3899825]

Middleton N, Yiallouros P, Kleanthous S, et al. A 10-year time-series analysis of respiratory and cardiovascular morbidity in Nicosia, Cyprus: the effect of short-term changes in air pollution and dust storms. Environ Health. 2008; 7:39.doi: 10.1186/1476-069X-7-39 [PubMed: 18647382]

Miller DB, Karoly ED, Jones JC, et al. Inhaled ozone (O3)-induces changes in serum metabolomic and liver transcriptomic profiles in rats. Toxicology and applied pharmacology. 2015; 286(2):65–79. S0041-008X(15)00116-7 [pii]. DOI: 10.1016/j.taap.2015.03.025 [PubMed: 25838073]

Miller DB, Snow SJ, Schladweiler MC, et al. Acute Ozone-Induced Pulmonary and Systemic Metabolic Effects are Diminished in Adrenalectomized Rats. Toxicol Sci. 2016; kfv331 [pii]. doi: 10.1093/toxsci/kfv331

Mons U, Muscat JE, Modesto J, Richie JP Jr, Brenner H. Effect of smoking reduction and cessation on the plasma levels of the oxidative stress biomarker glutathione - Post-hoc analysis of data from a smoking cessation trial. Free Radic Biol Med. 2016; 91:172–7. S0891-5849(15)01171-5 [pii]. DOI: 10.1016/j.freeradbiomed.2015.12.018 [PubMed: 26708755]

O'Rourke RW, White AE, Metcalf MD, et al. Systemic inflammation and insulin sensitivity in obese IFN-gamma knockout mice. Metabolism. 2012; 61(8):1152–61. S0026-0495(12)00046-7 [pii]. DOI: 10.1016/j.metabol.2012.01.018 [PubMed: 22386937]

Olefsky JM, Glass CK. Macrophages, inflammation, and insulin resistance. Annu Rev Physiol. 2010; 72:219–46. DOI: 10.1146/annurev-physiol-021909-135846 [PubMed: 20148674]

Rajagopalan S, Brook RD. Air pollution and type 2 diabetes: mechanistic insights. Diabetes. 2012; 61(12):3037–45. DOI: 10.2337/db12-0190 [PubMed: 23172950]

Author Manuscript Author Manuscript Author Manuscript Author Manuscript

Rich DQ, Mittleman MA, Link MS, et al. Increased risk of paroxysmal atrial fibrillation episodes associated with acute increases in ambient air pollution. Environmental health perspectives. 2006; 114(1):120–3. [PubMed: 16393668]

Ross R. Atherosclerosis--an inflammatory disease. N Engl J Med. 1999; 340(2):115–26. DOI: 10.1056/NEJM199901143400207 [PubMed: 9887164]

Ruidavets JB, Cournot M, Cassadou S, Giroux M, Meybeck M, Ferrieres J. Ozone air pollution is associated with acute myocardial infarction. Circulation. 2005; 111(5):563–9. DOI: 10.1161/01.CIR.0000154546.32135.6E [PubMed: 15699276]

Schultz MA, Abdel-Mageed AB, Mondal D. The nrf1 and nrf2 balance in oxidative stress regulation and androgen signaling in prostate cancer cells. Cancers (Basel). 2010; 2(2):1354–78. cancers2021354 [pii]. DOI: 10.3390/cancers2021354 [PubMed: 24281119]

Shah A, Mehta N, Reilly MP. Adipose inflammation, insulin resistance, and cardiovascular disease. JPEN J Parenter Enteral Nutr. 2008; 32(6):638–44. DOI: 10.1177/0148607108325251 [PubMed: 18974244]

Shimomura I, Funahashi T, Takahashi M, et al. Enhanced expression of PAI-1 in visceral fat: possible contributor to vascular disease in obesity. Nat Med. 1996; 2(7):800–3. [PubMed: 8673927]

Shoelson SE, Lee J, Yuan M. Inflammation and the IKK beta/I kappa B/NF-kappa B axis in obesity- and diet-induced insulin resistance. Int J Obes Relat Metab Disord. 2003; 27(Suppl 3):S49–52. DOI: 10.1038/sj.ijo.0802501 [PubMed: 14704745]

Srinivasan S, Avadhani NG. Cytochrome c oxidase dysfunction in oxidative stress. Free Radic Biol Med. 2012; 53(6):1252–63. S0891-5849(12)00416-9 [pii]. DOI: 10.1016/j.freeradbiomed.2012.07.021 [PubMed: 22841758]

Sun L, Liu C, Xu X, et al. Ambient fine particulate matter and ozone exposures induce inflammation in epicardial and perirenal adipose tissues in rats fed a high fructose diet. Part Fibre Toxicol. 2013; 10:43. 1743-8977-10-43 [pii]. doi: 10.1186/1743-8977-10-43 [PubMed: 23968387]

Sun Q, Hong X, Wold LE. Cardiovascular effects of ambient particulate air pollution exposure. Circulation. 2010; 121(25):2755–65. DOI: 10.1161/CIRCULATIONAHA.109.893461 [PubMed: 20585020]

Sun Q, Wang A, Jin X, et al. Long-term air pollution exposure and acceleration of atherosclerosis and vascular inflammation in an animal model. JAMA. 2005; 294(23):3003–10. DOI: 10.1001/jama.294.23.3003 [PubMed: 16414948]

Taube A, Schlich R, Sell H, Eckardt K, Eckel J. Inflammation and metabolic dysfunction: links to cardiovascular diseases. Am J Physiol Heart Circ Physiol. 2012; 302(11):H2148–65. DOI: 10.1152/ajpheart.00907.2011 [PubMed: 22447947]

Van Eeden S, Leipsic J, Paul Man SF, Sin DD. The relationship between lung inflammation and cardiovascular disease. American journal of respiratory and critical care medicine. 2012; 186(1):11–6. DOI: 10.1164/rccm.201203-0455PP [PubMed: 22538803]

Vella RE, Pillon NJ, Zarrouki B, et al. Ozone Exposure Triggers Insulin Resistance Through Muscle c-Jun N-Terminal Kinase Activation. Diabetes. 2015; 64(3):1011–24. db13-1181 [pii]. DOI: 10.2337/db13-1181 [PubMed: 25277399]

Wagner JG, Allen K, Yang HY, et al. Cardiovascular depression in rats exposed to inhaled particulate matter and ozone: effects of diet-induced metabolic syndrome. Environmental health perspectives. 2014; 122(1):27–33. DOI: 10.1289/ehp.1307085 [PubMed: 24169565]

Wallace TM, Levy JC, Matthews DR. Use and abuse of HOMA modeling. Diabetes Care. 2004; 27(6):1487–95. [PubMed: 15161807]

Weisberg SP, McCann D, Desai M, Rosenbaum M, Leibel RL, Ferrante AW Jr. Obesity is associated with macrophage accumulation in adipose tissue. J Clin Invest. 2003; 112(12):1796–808. DOI: 10.1172/JCI19246 [PubMed: 14679176]

Wellen KE, Hotamisligil GS. Inflammation, stress, and diabetes. J Clin Invest. 2005; 115(5):1111–9. DOI: 10.1172/JCI25102 [PubMed: 15864338]

Winer S, Winer DA. The adaptive immune system as a fundamental regulator of adipose tissue inflammation and insulin resistance. Immunol Cell Biol. 2012; 90(8):755–62. icb2011110 [pii]. DOI: 10.1038/icb.2011.110 [PubMed: 22231651]

Author Manuscript Author Manuscript Author Manuscript Author Manuscript

Xu H, Barnes GT, Yang Q, et al. Chronic inflammation in fat plays a crucial role in the development of obesity-related insulin resistance. J Clin Invest. 2003; 112(12):1821–30. DOI: 10.1172/JCI19451 [PubMed: 14679177]

Xu X, Yavar Z, Verdin M, et al. Effect of early particulate air pollution exposure on obesity in mice: role of p47phox. Arterioscler Thromb Vasc Biol. 2010; 30(12):2518–27. DOI: 10.1161/ATVBAHA.110.215350 [PubMed: 20864666]

Xu Z, Xu X, Zhong M, et al. Ambient particulate air pollution induces oxidative stress and alterations of mitochondria and gene expression in brown and white adipose tissues. Part Fibre Toxicol. 2011; 8:20.doi: 10.1186/1743-8977-8-20 [PubMed: 21745393]

Yang CH, Wei L, Pfeffer SR, et al. Identification of CXCL11 as a STAT3-dependent gene induced by IFN. Journal of immunology. 2007; 178(2):986–92.

Yang Y, Dieter MZ, Chen Y, Shertzer HG, Nebert DW, Dalton TP. Initial characterization of the glutamate-cysteine ligase modifier subunit Gclm(−/−) knockout mouse. Novel model system for a severely compromised oxidative stress response. J Biol Chem. 2002; 277(51):49446–52. M209372200 [pii]. DOI: 10.1074/jbc.M209372200 [PubMed: 12384496]

Ying Z, Allen K, Zhong J, et al. Subacute inhalation exposure to ozone induces systemic inflammation but not insulin resistance in a diabetic mouse model. Inhalation toxicology. 2016; 28(4):155–63. DOI: 10.3109/08958378.2016.1146808 [PubMed: 26986950]

Yuan M, Konstantopoulos N, Lee J, et al. Reversal of obesity- and diet-induced insulin resistance with salicylates or targeted disruption of Ikkbeta. Science. 2001; 293(5535):1673–7. DOI: 10.1126/science.1061620 [PubMed: 11533494]

Zheng Z, Xu X, Zhang X, et al. Exposure to ambient particulate matter induces a NASH-like phenotype and impairs hepatic glucose metabolism in an animal model. J Hepatol. 2013; 58(1):148–54. DOI: 10.1016/j.jhep.2012.08.009 [PubMed: 22902548]

Zhong J, Rao X, Deiuliis J, et al. A potential role for dendritic cell/macrophage-expressing DPP4 in obesity-induced visceral inflammation. Diabetes. 2013; 62(1):149–57. db12-0230 [pii]. DOI: 10.2337/db12-0230 [PubMed: 22936179]

Author Manuscript Author Manuscript Author Manuscript Author Manuscript

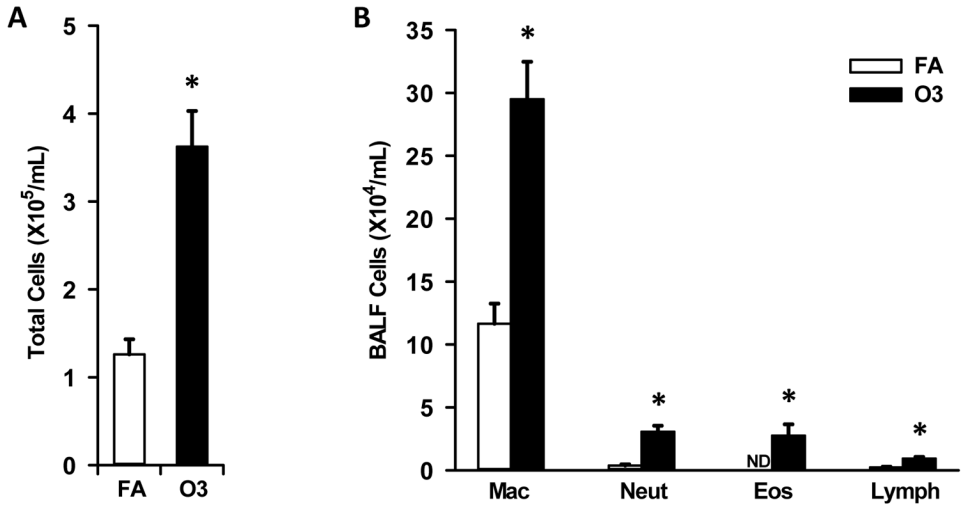

Figure 1. Effect of O_3 exposure on bronchoalveolar cellularity

Total cells (A) and inflammatory cell differentials (B) were enumerated in bronchoalveolar lavage fluid as described in Methods. ND - not detected; * indicates significantly different from filtered air (FA) exposed mice; $p<0.05$.

Author Manuscript Author Manuscript Author Manuscript Author Manuscript

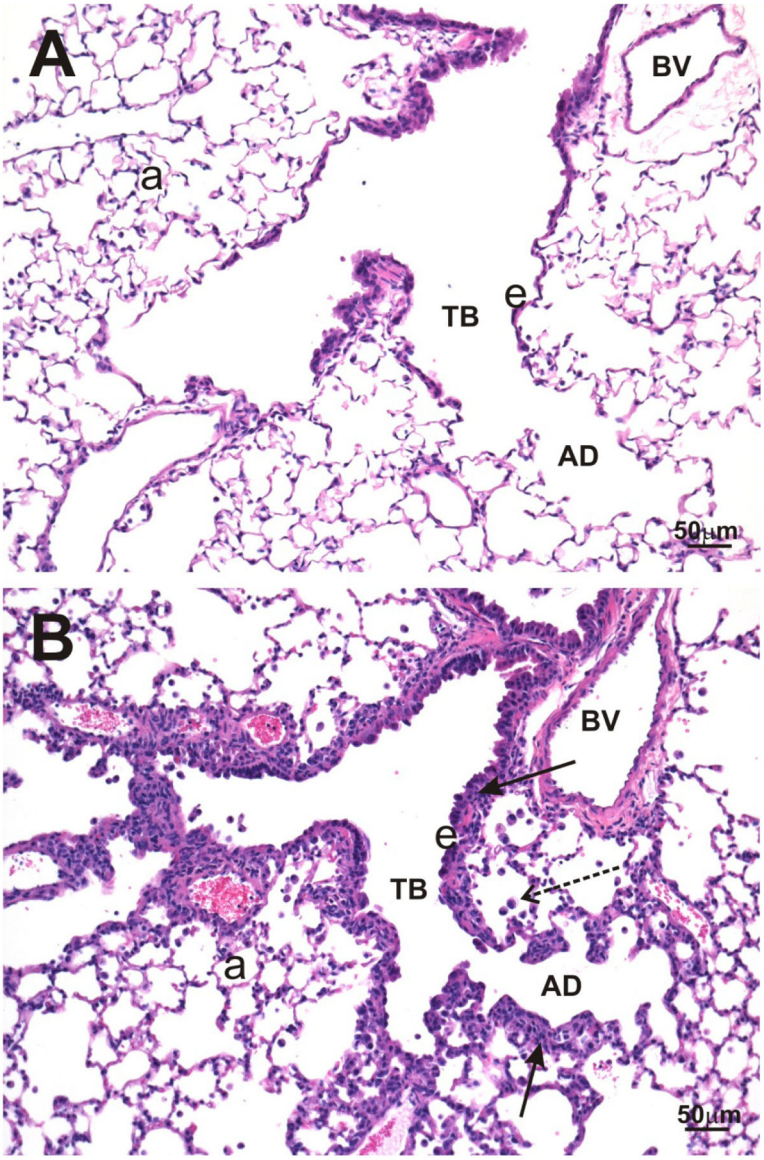

Figure 2. Effect of O_3 exposure on pulmonary histopathology

Light photomicrographs of lung tissue from KK mice exposed to filtered air (A) or 0.5 ppm O_3 (B). No exposure-related lung lesions are present in the centriacinar region of the lung from a control mouse exposed only to filtered air (A). In contrast, airway walls (solid arrows) of terminal bronchioles (TB) and alveolar ducts (AD), in the centriacinus of the lung, from an O_3-exposed mouse (B) are markedly thickened due to hyperplasia/hypertrophy of surface epithelium (e), intramural fibrosis, smooth muscle hypertrophy, and an influx of mixed inflammatory cells. Small aggregates of monocytes/macrophages (stippled arrow) are also present in alveolar airspaces in B. a, alveolar parenchyma. Tissue sections were stained with hematoxylin and eosin.

Author Manuscript Author Manuscript Author Manuscript Author Manuscript

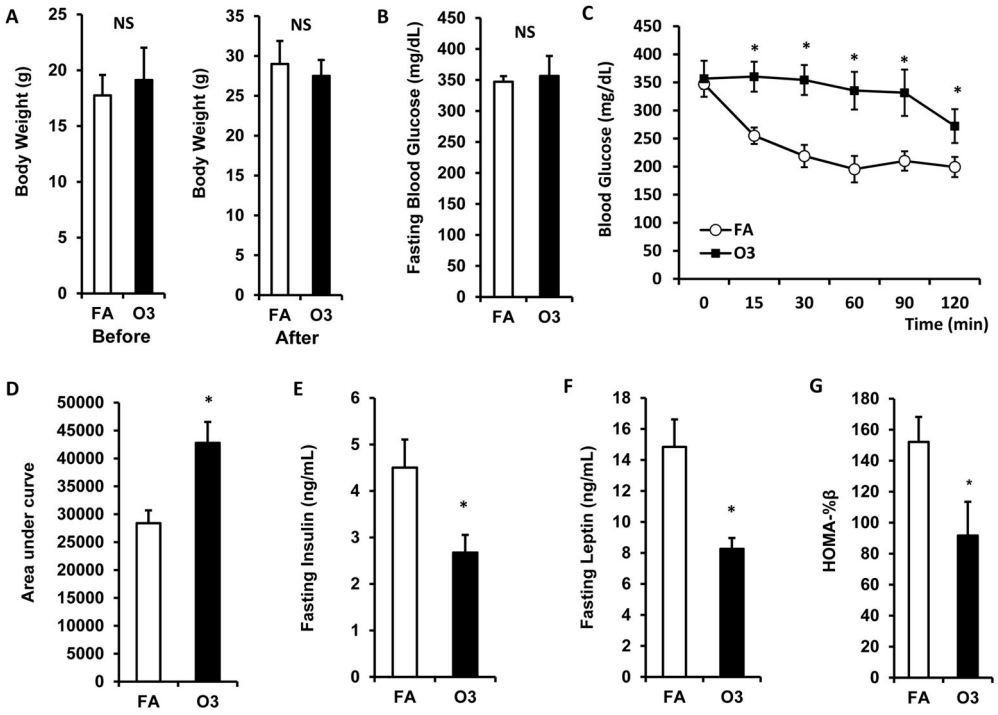

Figure 3. O_3 exposure impaired insulin sensitivity

KK mice were exposed to O_3 or FA for 13 days. Body weight was measured before and after exposure (A). ITT was performed 1 day after the last exposure. Blood glucose level was detected before and 0, 15, 30, 60, 90, 120 min after i.p. injection of 0.75U/kg body weight insulin (B, fasting blood glucose; C, blood glucose level upon insulin injection; D, area under curve). Plasma was used for the detection of insulin (E) and leptin (F). n=8; *, $p<0.05$.

Author Manuscript Author Manuscript Author Manuscript Author Manuscript

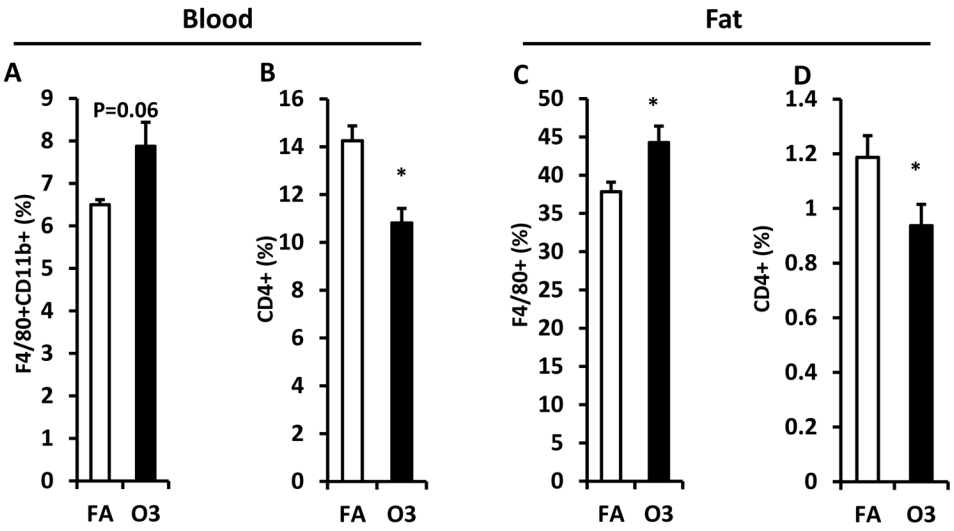

Figure 4. Effect of O_3 exposure on macrophages and $CD4^+$ T cells

White blood cells isolated from peripheral blood and SVF harvested from epididymal fat were used for the flow cytometric detection of macrophage and T cell population. Percentage of macrophage in blood ($F4/80^+$ $CD11b^+$, A) and epididymal fat ($F4/80^+$, C) was shown. CD4+ T cells in blood (B) and epididymal fat (D) were also detected. n=8; *, $p<0.05$.

Author Manuscript Author Manuscript Author Manuscript Author Manuscript

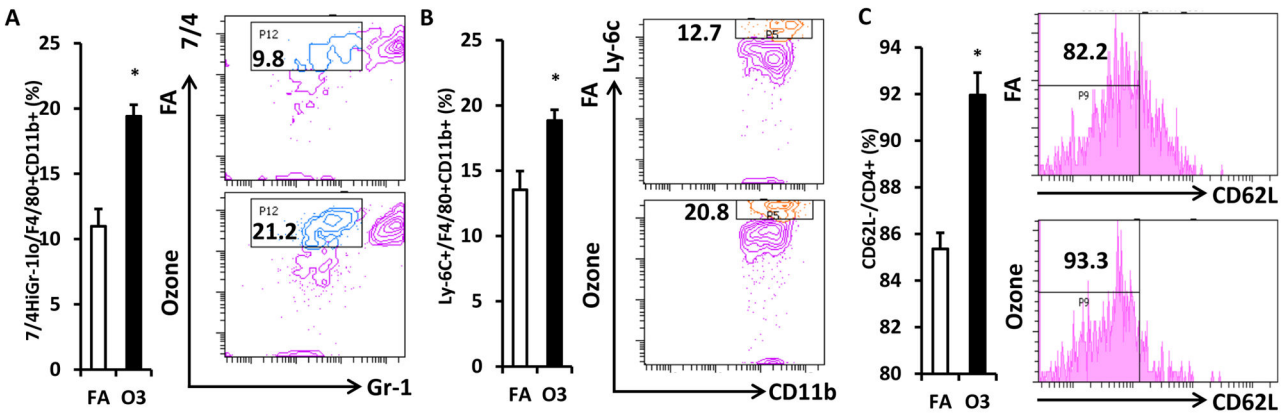

Figure 5. Impact of O_3 exposure on activation of circulating macrophages and $CD4^+$ T cells

White blood cells isolated from peripheral blood were used for the flow cytometric detection of macrophage and T cell activation. $F4/80^+$ $CD11b^+$ macrophages were gated for the analysis of inflammatory marker. Inflammatory macrophages as evidenced by $7/4^{high}$ $Gr\text{-}1^{low}$ (A) or $Ly\text{-}6C^+$ (B) were analyzed (Left, statistical analysis; Right, representative images). $CD4^+$ cells were gated for the detection of T cell activation. Activated $CD4^+$ T cells ($CD4^+$ $CD62L^-$) were shown (C; Left, statistical analysis; Right, representative images). n=8; *, $p<0.05$.

Author Manuscript Author Manuscript Author Manuscript Author Manuscript

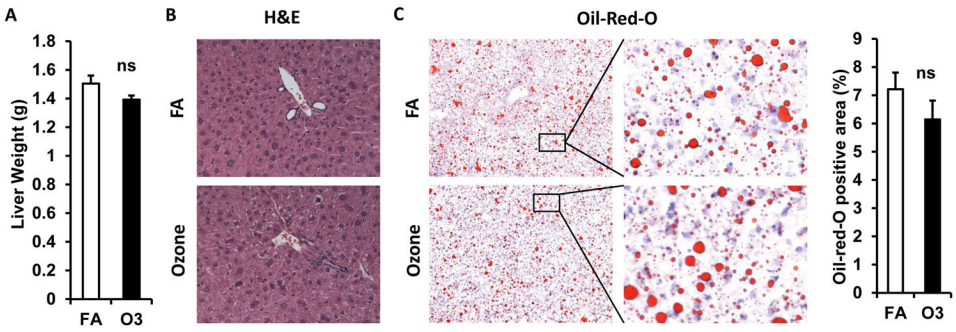

Figure 6. Effect of O_3 exposure on liver weights and lipid content

A, Liver weight of FA- or O_3-exposed mice; B, Sections of liver were used for the H&E staining and representative images were shown; C, Oil-Red-O staining of frozen liver sections (Left, statistical analysis; Right, representative images).

Author Manuscript Author Manuscript Author Manuscript Author Manuscript

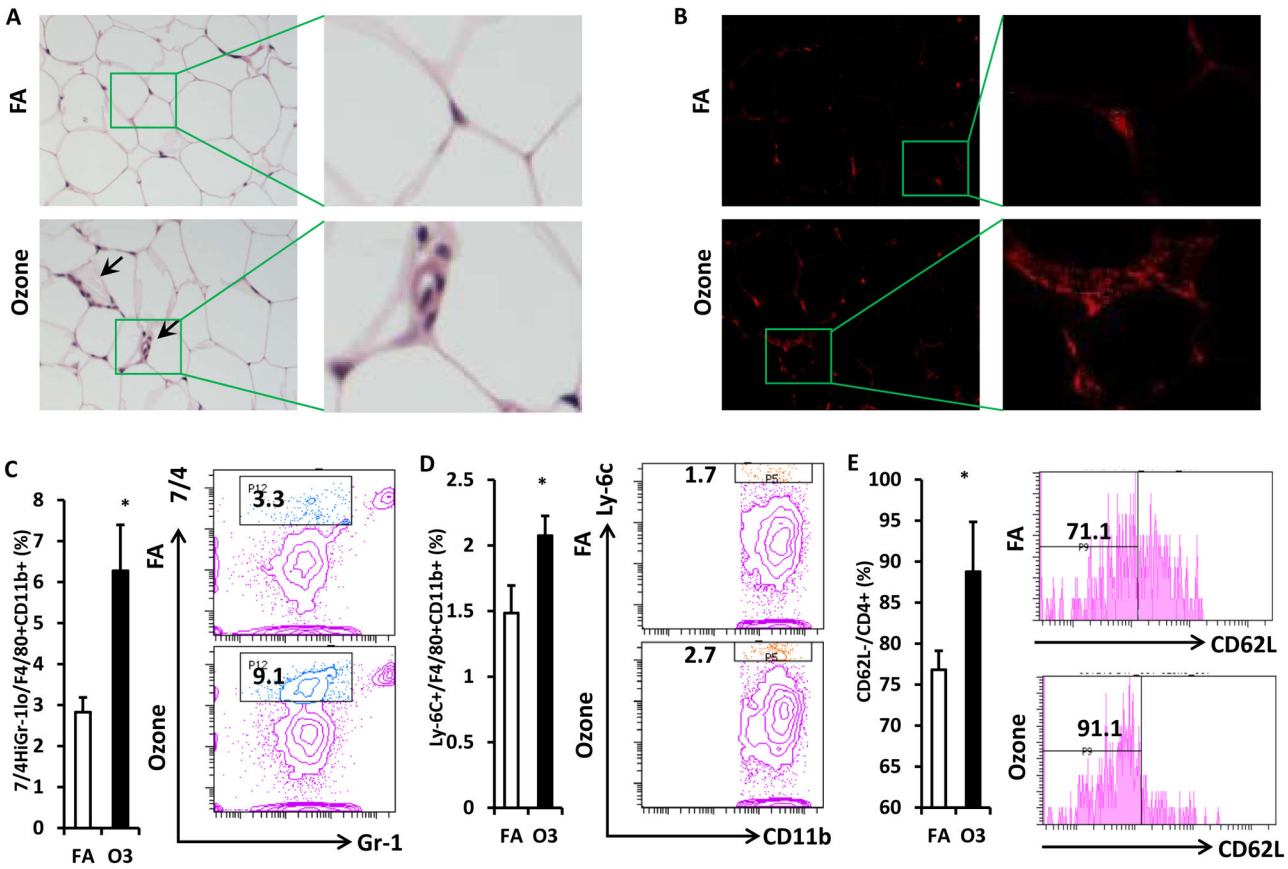

Figure 7. O_3 exposure promoted activation of macrophages and $CD4^+$ T cells in visceral adipose tissue

Sections of epididymal fat were used for the H&E staining (A) and immunofluorescence staining (B, CD11b). Representative images were shown (arrows indicate crown-like structure infiltrated by inflammatory cells/macrophages). SVF harvested from epididymal fat was used for the flow cytometric detection of macrophage and T cell activation. $F4/80^+$ macrophages were gated for the analysis of inflammatory marker. Inflammatory macrophages as evidenced by $7/4^{high}$ $Gr\text{-}1^{low}$ (C) or $Ly\text{-}6C^+$ (D) were analyzed (Left, statistical analysis; Right, representative images). $CD4^+$ cells were gated for the detection of T cell activation. Activated $CD4^+$ T cells ($CD4^+$ $CD62L^-$) were shown (E; Left, statistical analysis; Right, representative images). n=8; *, $p<0.05$.

Author Manuscript Author Manuscript Author Manuscript Author Manuscript

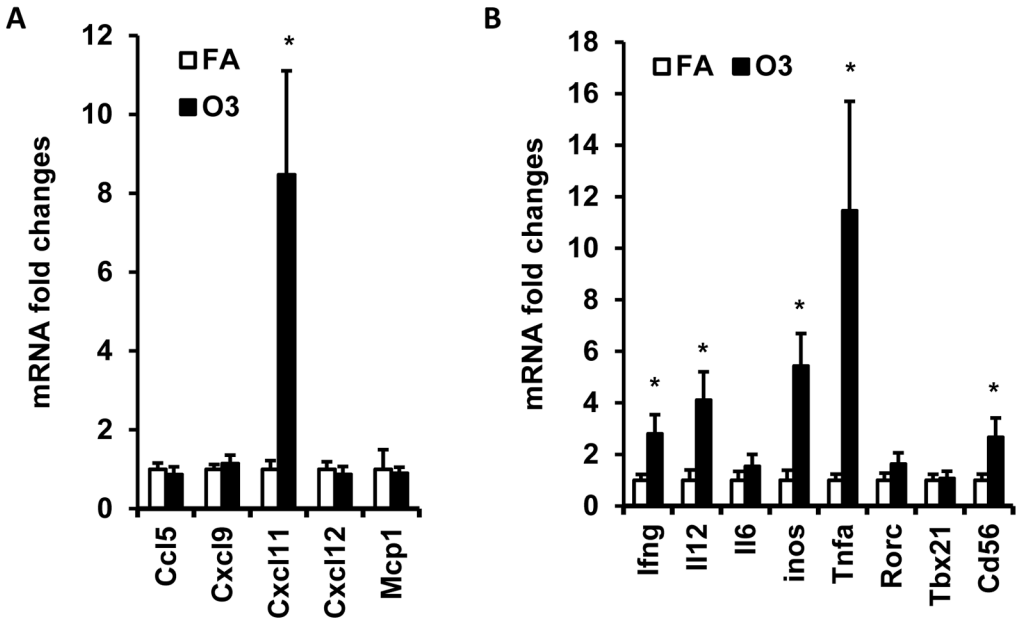

Figure 8. Effect of O_3 exposure on inflammatory gene expression in visceral adipose tissue

Epididymal fat of mice exposed to filtered air (FA) or O_3 was used for real-time PCR detection of inflammatory gene expression. mRNA expression of chemokines(A, *Ccl5*, *Cxcl9*, *Cxcl11*, *Cxcl12*, and *Mcp1*) and inflammatory genes (B, *Ifng*, *Il12*, *Il6*, *Inos*, *Tnfa*, *Rorc*, *Tbx21* and *Cd56*) was shown. N=8/group; *, $p<0.05$.

Author Manuscript Author Manuscript Author Manuscript Author Manuscript

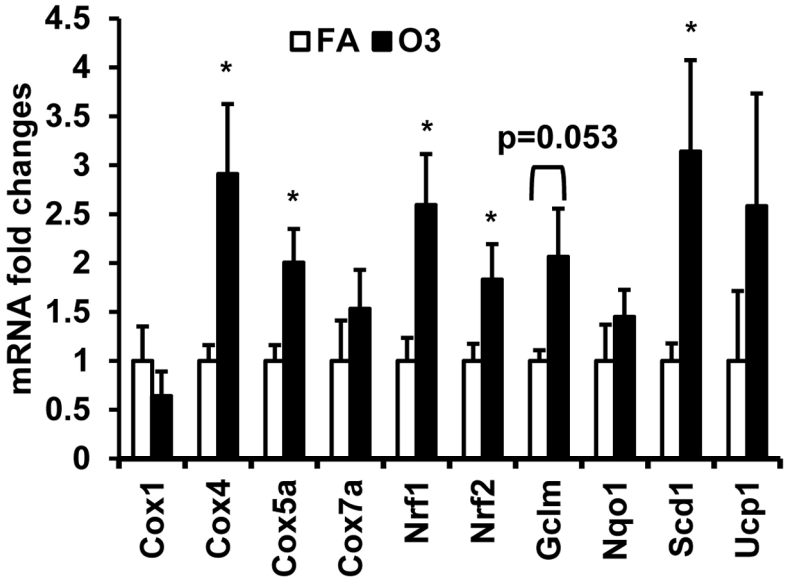

Figure 9. O_3 exposure induces expression of cyclooxygenase (COX) and oxidative stress response in VAT

Epididymal fat of mice exposed to filtered air FA or O_3 was used for real-time PCR detection of genes involved in oxidative stress: *Cox1*, *Cox4*, *Cox5a*, *Cox7a*, *Scd1*, *Nrf1*, *Nrf2*, *Gclm*, *Noq1*, and *Ucp1*. *, $p<0.05$.

Author Manuscript Author Manuscript Author Manuscript Author Manuscript

Table 1

Real-time PCR primer sequence

Target Gene	Primer Sequence (5′ to 3′)
TNFα	Forward CAACGGCATGGATCTCAAAGAC
	Reverse AGATAGCAAATCGGCTGACGGT
MCP-1	Forward TCACCTGCTGCTACTCATTCACCA
	Reverse TACAGCTTCTTTGGGACACCTGCT
CCL5	Forward CTCACCATCATCCTCACTGC
	Reverse AAATACTCCTTGACGTGGGC
CXCL-12	Forward TCTGCATCAGTGACGGTAAAC
	Reverse TGAAGGGCACAGTTTGGAG
CXCL-9	Forward TCCGCTGTTCTTTTCCTCTTG
	Reverse GAGGGATTTGTAGTGGATCGTG
CXCL-11	Forward ATGGCAGAGATCGAGAAAGC
	Reverse GCACCTTTGTCGTTTATGAGC
RORγ	Forward ATGTCTGCAAGTCCTTCCG
	Reverse CTCCCACATTGACTTCCTCTG
T-bet	Forward TTCAACCAGCACCAGACAG
	Reverse AGACCACATCCACAAACATCC
iNOS	Forward CCAGTTGTGCATCGACCTAG
	Reverse TCACCTCCAACACAAGATCAG
IFNγ	Forward TCTTCCTCATGGCTGTTTCTG
	Reverse CACCATCCTTTTGCCAGTTC
IL-12	Forward ACAGATGACATGGTGAAGACG
	Reverse TCGTTCTTGTGTAGTTCCAGTG
IL-6	Forward ATCCAGTTGCCTTCTTGGGACTGA
	Reverse TAAGCCTCCGACTTGTGAAGTGGT
COX1	Forward AGGAGATGGCTGCTGAGTTGG
	Reverse AATCTGACTTTCTGAGTTGCC
COX4	Forward AGCCATTTCTACTTCGGTGTG
	Reverse GCAGACAGCATCGTGACAT
COX5	Forward GGGTCACACGAGACAGATGA
	Reverse GGAACCAGATCATAGCCAACA
COX7	Forward GCTGCTGAGGACGCAAAATGAGG
	Reverse CCATTCCCCCGCCTTTCAAG
SCD1	Forward GTCAGGAGGGCAGGTTTC
	Reverse GAGCGTGGACTTCGGTTC
Nrf1	Forward GAACTGCCAACCACAGTCAC
	Reverse TTTGTTCCACCTCTCCATCA
Nrf2	Forward TCACACGAGATGAGCTTAGGGCAA
	Reverse TACAGTTCTGGGCGGCGACTTTAT
Gclm	Forward CCACCAGATTTGACTGCCTTTGCT

Author Manuscript

Author Manuscript

Author Manuscript

Author Manuscript

Target Gene	Primer Sequence (5′ to 3′)
NQO1	Reverse AATCCTGGGCTTCAATGTCAGGGA
	Forward ATGGCATCCAGTCCTCCATCAAGA
	Reverse ACAAGTTAGTCCCTCGGCCATTGT
UCP1	Forward ACTGCCACACCTCCAGTCATT
	Reverse CTTTGCCTCACTCAGGATTGG
β-actin	Forward TGTGATGGTGGGAATGGGTCAGAA
	Reverse TGTGGTGCCAGATCTTCTCCATGT